NATIONAL ADVISORY COMMITTEE FOR AERONAUTICS

TECHNICAL NOTE

No. 1814

EFFECTS OF SEVERAL DESIGN VARIABLES ON TURBINE-WHEEL WEIGHT

By Vincent L. LaValle and Merle C. Huppert

Lewis Flight Propulsion Laboratory
Cleveland, Ohio

Washington
February 1949

NATIONAL ADVISORY COMMITTEE FOR AERONAUTICS

TECHNICAL NOTE NO. 1814

EFFECTS OF SEVERAL DESIGN VARIABLES ON TURBINE-WHEEL WEIGHT

By Vincent L. LaValle
and Merle C. Huppert

SUMMARY

An analysis is presented to show the effect of several design variables on turbine-wheel weight. A model wheel was selected based on the de Laval equation for a disk of uniform strength. Equations were developed for the calculation of weights of the disk, the rim, and the blades, involving as variables the blading aspect ratio and solidity, the ratio of the centrifugal stress at the blade roots to that in the disk (stress ratio), and the ratio of wheel diameter at the blade root to wheel diameter at the blade tip (diameter ratio). The effect of changes in these variables on total wheel weight and disk weight is presented, as well as the effect of changes in diameter ratio, aspect ratio, and solidity on blade weight.

For a turbine wheel with a blade-annulus area of 2 square feet, a blading aspect ratio of 2, a stress ratio of 0.9, and a blading solidity of 1.85, changes in the diameter ratio caused the greatest change in wheel weight. Increasing the diameter ratio from 0.70 to 0.80 approximately doubled wheel weight; however, increasing diameter ratio increased the allowable tip speed for a given stress at the blade root.

The variation of diameter ratio and aspect ratio had the greatest effect on wheel weight within the range chosen for the variables.

An increase of stress ratio and blading solidity increased total wheel weight, stress ratio having a greater effect on total wheel weight than solidity.

INTRODUCTION

In the preliminary stages of engine design or in a comparative evaluation of various types of power plant, it is desirable to have a method of obtaining the approximate weights of the various engine components. Cycle analysis will establish cycle efficiencies and power output per pound of air, and aerodynamic studies of the gas-turbine engine will establish air-flow capacity for specified sizes of gas-turbine components. The establishment of proper relations among weight of gas-turbine components, areas of flow passages, pressure ratios, and operating temperatures has not, however, been reduced to a rational process. Stator- and rotor-weight power ratios are discussed in reference 1 in terms of stage efficiencies and bending stresses at the blade root; however, only compressors are considered and the presentation is not detailed. Other methods have been developed to relate turbine geometry to performance whereby the significant geometric turbine dimensions, insofar as thermodynamic and aerodynamic properties are concerned, may be determined.

An analysis was conducted at the NACA Lewis laboratory to relate these significant geometric dimensions of the turbine to wheel weight. A comparison is made to show the agreement between the calculated and observed weights of turbine wheels. Variation of wheel weight with variation of annulus area and diameter ratio is presented for a representative set of values of aspect ratio, solidity, and ratio of stress in the blade to stress in the disk.

SYMBOLS

The following symbols are used in the analysis:

A	annulus flow area behind rotor, (sq ft)
A_b	cross-sectional area of blade at any radius r_b, (sq ft)
A_i	cross-sectional area of blade at its root, (sq ft)
A_o	cross-sectional area of blade at its tip, (sq ft)
b	radial rim thickness, (fig. 1), (ft)
b_x	axial rim thickness, (fig. 1), (ft)
D_i	wheel diameter at blade root, (ft)
D_o	wheel diameter at blade tip, (ft)
D_i/D_o	diameter ratio
exp	base of Napierian logarithmic system e raised to power in parentheses following exp

1064

F	centrifugal force at any radius r_b, (lb)
F_b	centrifugal force of blade, (lb)
F_r	centrifugal force of rim, (lb)
F_T	total centrifugal force, (lb)
f	area ratio, A_o/A_i
g	acceleration due to gravity, 32.2 (ft/sec^2)
K	proportionality constant, $(A_i/b_x{}^2)$
l	blade length, (fig. 1), (ft)
N	number of blades
n	factor used for defining blade-area distribution
r	disk radius, (fig. 1), (ft)
r_b	any radius along blade length, (ft)
r_i	radius to blade root (outer radius of rim), (fig. 1), (ft)
r_o	radius to blade tip (outer radius of wheel), (fig. 1), (ft)
r_r	inner radius of rim, (fig. 1), (ft)
s_b	blade stress, (lb/sq ft)
s_d	disk stress, (lb/sq ft)
s_b/s_d	stress ratio
t	axial thickness of disk tip at r_r, (fig. 1), (ft)
V_p	velocity at blade pitch section, (ft/sec)
V_t	wheel tip velocity, (ft/sec)
W_b	blade weight, (lb)
W_d	disk weight, (lb)
W_r	rim weight, (lb)

W_T total wheel weight, (lb)

y disk thickness at any radius r, (fig. 1), (ft)

y_a disk thickness at center of rotation, (fig. 1), (ft)

$\beta = \dfrac{1 + D_i/D_o}{1 - D_i/D_o} = \dfrac{A}{\pi l^2}$

δ aspect ratio, (l/b_x)

$\epsilon = b_x/t$

ρ_b blade density, (lb/cu ft)

ρ_d disk density, (lb/cu ft)

σ blade solidity, (b_x/τ)

τ blade pitch, (ft)

ψ stress correction factor

ω angular velocity, (radians/sec)

BASIS OF ANALYSIS

The basis of this analysis was a wheel model composed of a disk, a rim, and a blade section, as shown in figure 1.

The disk-section profile of the model is defined by the equation

$$y = y_a \exp\left(\frac{-\rho_d \, \omega^2 \, r^2}{2 \, s_d \, g}\right) \qquad (1)$$

Disks of this type were used by designers of de Laval wheels (reference 2) and are in accordance with the design practice used for some current wheels.

The rim of the wheel was assumed to have a square cross section with the rim thickness in the axial direction equal to the axial dimension of the blade at its root.

1064

In order to arrive at a value of the thickness of the disk at the rim, the rim was assumed to be divided into separate segments by radial cuts. This condition is closely approached by turbines that use fir-tree attachments or any attachment system in which the rim is slotted. This assumption was made to find $\epsilon = b_x/t$, which is defined as the ratio of the axial rim thickness to the axial thickness of the disk at the inner radius of the rim.

The only stresses considered in the disk and the blades were those caused by centrifugal force. Vibratory and bending stresses under certain conditions may become important but their consideration is beyond the scope of this report. Stresses due to temperature gradients in the wheel are likewise neglected.

In the consideration of the cross-sectional area of the blade at its root, it was assumed that this area would be equal to a constant times the width of the rim squared or $A_1 = K\, b_x^2$.

ANALYSIS

On the basis of the model chosen (fig. 1), the weights of the disk, the rim, and the blades may be computed as follows:

Disk Weight

Equation (1), which defines the profile of a disk of uniform strength, is used as the basis of the analysis.

$$y = y_a \exp\left(\frac{-\rho_d\, \omega^2\, r^2}{2\, s_d\, g}\right) \tag{1}$$

The weight of an annular element of the disk is

$$dW_d = 2\pi y\, \rho_d\, r\, dr$$

Integrating between the distance to the rim of the wheel r_r and zero yields

$$W_d = \frac{\pi\, y_a\, \rho_d \left[\exp\left(\frac{-\rho_d\, \omega^2\, r_r^{\,2}}{2\, s_d\, g}\right) - 1\right]}{-\frac{\rho_d\, \omega^2}{2\, s_d\, g}}$$

From equation (1) when $y = t$ and $r = r_r$,

$$y_a = t \exp\left(\frac{\rho_d \, \omega^2 \, r_r^{\,2}}{2 \, s_d \, g}\right)$$

then

$$W_d = \frac{\pi \, \rho_d \, t \left[\exp\left(\frac{\rho_d \, \omega^2 \, r_r^{\,2}}{2 \, s_d \, g}\right) - 1\right]}{\frac{\rho_d \, \omega^2}{2 \, s_d \, g}} \tag{2}$$

In order to eliminate ω, r_r, and t from equation (2) to get the disk weight in terms of the following variables, stress ratio, diameter ratio, solidity, and aspect ratio, a relation is first derived for the blade stress due to centrifugal force for a blade taper of the following type

$$\frac{r_b - r_i}{r_o - r_i} = \left(\frac{A_b - A_i}{A_o - A_i}\right)^n \tag{3}$$

where n is a factor that defines the variation of the cross-sectional area from the root to the tip of the blade; for example, when $n = 1$ the taper is linear and when $n = 2$ the taper is parabolic. Then

$$r_b = r_i + l \left(\frac{A_b - A_i}{A_o - A_i}\right)^n \tag{4}$$

$$dr_b = \frac{ln}{(A_o - A_i)^n} \, (A_b - A_i)^{n-1} \, dA_b \tag{5}$$

The centrifugal force at any radius r_b due to an elemental volume of blade is equal to

$$dF = \frac{\rho_b \, \omega^2 \, A_b \, r_b \, dr_b}{g} \tag{6}$$

and the blade stress at its root is

$$s_b = \frac{\int_{A_i}^{A_o} dF}{A_i} \tag{7}$$

Substituting equations (4), (5), and (6) in equation (7) and integrating yields

$$s_b = \frac{\rho_b \omega^2 (r_o - r_i)}{g}\left\{r_i\left(\frac{n}{n+1}\,\frac{A_o - A_i}{A_i}+1\right) + (r_o - r_i)\left[\frac{n(A_o-A_i)}{(2n+1)A_i}+\frac{1}{2}\right]\right\}$$

When f is substituted for A_o/A_i and the preceding equation is rearranged,

$$s_b = \frac{\rho_b \omega^2 r_o^2}{g}\left[1-\left(\frac{D_i}{D_o}\right)^2\right]\left(\frac{1}{1+\frac{D_i}{D_o}}\right)\left\{\left[\frac{n}{2n+1}(f-1)+\frac{1}{2}\right]+\frac{D_i}{D_o}\left[\frac{n^2(f-1)}{(n+1)(2n+1)}+\frac{1}{2}\right]\right\}$$

Let

$$\psi = \frac{2}{1+\frac{D_i}{D_o}}\left\{\left[\frac{n}{2n+1}(f-1)+\frac{1}{2}\right]+\frac{D_i}{D_o}\left[\frac{n^2(f-1)}{(n+1)(2n+1)}+\frac{1}{2}\right]\right\}$$

then

$$s_b = \frac{\rho_b \omega^2 r_o^2}{2g}\left[1-\left(\frac{D_i}{D_o}\right)^2\right]\psi \tag{8}$$

This equation gives the stress at the root of a blade for different blade-area distributions. The symbol ψ represents the ratio of the stress in a tapered blade to the stress in a parallel-sided blade. When $\psi = 1$, the equation gives the stress at the root of a parallel-sided blade.

In figure 2, ψ is plotted against area ratio f for values of diameter ratio D_i/D_o of 0.6, 0.7, and 0.8, and for three blade cross-sectional area distributions, $n = 1$ (linear taper), $n = 2$ (parabolic taper), and $n = 3/2$. A plot of blade tip velocity V_t against diameter ratio D_i/D_o for four different values of s_b/ψ is presented in figure 3. Figure 4 is similar to figure 3 except that the ordinate is blade pitch velocity V_p, which is useful in calculations of turbine power.

From figure 2 if f, D_i/D_o, and n are known, ψ can be determined; then from figure 3 if s_b is known, the allowable blade tip velocity V_t can be found.

When the following relations for r_o and β are substituted in equation (8)

$$r_o = \frac{l}{1 - \frac{D_i}{D_o}}, \quad \text{and} \quad \beta = \frac{1 + \frac{D_i}{D_o}}{1 - \frac{D_i}{D_o}} = \frac{A}{\pi l^2}$$

then equation (8) yields

$$s_b = \frac{\rho_b \omega^2 l^2 \psi\beta}{2g} \tag{9}$$

$$F_b = s_b A_i N$$

$$= \frac{\rho_b \omega^2 l^2 \psi \beta A_i N}{2g}$$

It may be assumed that the cross-sectional area of the blade at the root is equal to a constant times b_x^2 or

$$A_i = Kb_x^2$$

and the number of blades

$$N = \frac{\pi(r_o + r_i)\,\sigma}{b_x}$$

When it is also assumed that the rim of the wheel is square in cross section,

$$\delta = \frac{l}{b} = \frac{l}{b_x}$$

then

$$F_b = \frac{\rho_b \omega^2 l^4 \psi\beta^2 K \pi \sigma}{2g\delta} \tag{10}$$

The rim of the model was assumed to be separated into segments by radial cuts in order to arrive at a value of the thickness of the disk at the rim. Then

$$F_r = \frac{\pi}{2} (2r_o - 2l - b)^2 b_x b \rho_d \frac{\omega^2}{g}$$

$$= \frac{\pi \rho_d l^4 \omega^2}{2\delta^2 g} \left(\beta - 1 - \frac{1}{\delta}\right)^2 \tag{11}$$

The centrifugal force acting at r_r is the sum of equations (10) and (11) and is equal to

$$F_T = \frac{\rho_b \omega^2 l^4 \psi \beta^2 K \pi \sigma}{2g\delta} + \frac{\pi \rho_d l^4 \omega^2}{2\delta^2 g} \left(\beta - 1 - \frac{1}{\delta}\right)^2 \tag{12}$$

The centrifugal force acting at r_r is also equal to the area at r_r times the stress at r_r.

$$F_T = 2 \pi r_r t s_d \tag{13}$$

Combining equations (2), (12), and (13) and using

$$r_r = r_o - l - b$$

$$= \frac{l}{2} \left(\beta - 1 - \frac{2}{\delta}\right)$$

yields the final form of the disk-weight formula

$$W_d = \frac{\pi\, l^3\, \rho_b}{\delta\left(\beta-1-\frac{2}{\delta}\right)}\left[\psi K\sigma\beta^2 + \frac{\rho_d\left(\beta-1-\frac{1}{\delta}\right)^2}{\rho_b\delta}\right]\left\{\exp\left[\frac{\rho_d}{\rho_b}\,\frac{s_b}{s_d}\,\frac{\left(\beta-1-\frac{2}{\delta}\right)^2}{4\psi\beta}\right] - 1\right\} \tag{14}$$

When equations (9), (12), and (13) are combined, an equation is developed for $\epsilon = b_x/t$, defined as the ratio of the axial rim thickness to the axial thickness of the disk at the inner radius of the rim. Then

$$\epsilon = \frac{b_x}{t} = \frac{s_d}{s_b}\,\frac{\left(\beta - 1 - \frac{2}{\delta}\right)\beta\,\psi}{\left[\frac{\rho_d}{\delta\rho_b}\left(\beta - 1 - \frac{1}{\delta}\right)^2 + \beta^2\,\psi K\sigma\right]} \tag{15}$$

In equation (14)

$$\exp\left[\frac{\rho_d}{\rho_b}\,\frac{s_b}{s_d}\,\frac{\left(\beta - 1 - \frac{2}{\delta}\right)^2}{4\,\psi\,\beta}\right] = \frac{y_a}{t} \tag{15a}$$

This expression in conjunction with equation (15) may be used for determining wheel proportions.

Blade Weight

The total blade weight is

$$W_b = N\int_{r_i}^{r_o}\rho_b\,A_b\,dr_b \tag{16}$$

By use of equation (5) and integration between A_o and A_i, equation (16) becomes

$$W_b = \frac{\rho_b\,Nn\,(r_o - r_i)}{(A_o - A_i)^n}\left[\frac{1}{n+1}(A_o - A_i)^{n+1} + \frac{A_i}{n}(A_o - A_i)^n\right] \tag{17}$$

1064

Clearing and rearranging equation (17) yields

$$W_b = \frac{\rho_b K l \sigma A}{\delta}\left[\frac{n(f-1)}{n+1} + 1\right] \tag{18}$$

For a linearly tapered blade where $n = 1$

$$W_b = \frac{\rho_b K l \sigma A}{\delta}\left(\frac{f+1}{2}\right) \tag{19}$$

Rim Weight

With reference to figure 1, the weight of the rim, assuming that it has a square cross section (that is, $b = b_x$) is

$$W_r = 2\pi\left(r_o - l - \frac{b}{2}\right)b^2 \rho_d$$

Clearing and rearranging yields

$$W_r = \frac{\pi l^3 \rho_d}{\delta^2}\left(\beta - 1 - \frac{1}{\delta}\right) \tag{20}$$

RESULTS AND DISCUSSION

In order to illustrate the effect of each variable on turbine-wheel weight, calculations were made applying values to the variables consistent with those of some current turbines.

The weights of the disk, blades, and rim were calculated by the use of equations (14), (19), and (20), respectively, and then added to obtain the total wheel weight.

Plots that show the effect of the variables considered on disk weight, blade weight, and total wheel weight are shown in figures 5, 6, and 7, respectively. In the computation of the data for these figures, representative values were assigned to the diameter ratio, the aspect ratio, the stress ratio, and the solidity. While one factor was being investigated, the other variables were maintained constant at an assigned basic value.

The basic values assigned to each variable being investigated and the range of the variable investigated are listed in the following table:

Variable	Basic value	Range
D_i/D_o	0.700	0.600 - 0.800
δ	2.000	1.500 - 3.500
s_b/s_d	.900	.700 - 1.100
σ	1.850	1.250 - 2.300

The constants were as follows:

Area ratio, f 0.3
Annulus area, A, sq ft 2
Proportionality constant, K 0.15
Blade density, ρ_b, lb/cu ft 540
Disk density, ρ_d, lb/cu ft 510

Curves of calculated values of disk weight, as affected by the four variables, diameter ratio D_i/D_o, aspect ratio δ, stress ratio s_b/s_d, and solidity σ, are shown in figure 5. For comparison purposes the abscissas are so arranged that the basic values of the variables intersect at a common wheel-weight point. With diameter ratio as the variable and aspect ratio, solidity, and stress ratio constant, it may be seen that a change of diameter ratio from the basic point of 0.70 to 0.80 causes an increase in disk weight of more than 200 percent; however, with a fixed stress at the blade root, increasing the diameter ratio increases the allowable tip velocity as shown in figure 3. A change in aspect ratio from 1.5 to 3.5 caused a disk-weight increase of almost 72 percent. A change in stress ratio from 0.7 to 1.1 caused an increase in disk weight of about 65 percent. Solidity, over its range, had a smaller effect on disk weight than the other variables, increasing the disk weight about 23 percent over its range of from 1.25 to 2.3.

The effects of varying diameter ratio, aspect ratio, and solidity on blade weight are shown in figure 6. Over the entire range chosen for these variables, the blade weight was decreased about 40 percent by an increase in diameter ratio of 0.60 to 0.80 and about 79 percent by an increase in aspect ratio of 1.5 to 3.2. The effect of increasing the solidity from 1.0 to 2.0 was to increase blade weight about 54 percent.

Curves of calculated values of total wheel weight, as affected by the four variables, diameter ratio, aspect ratio, stress ratio, and solidity, are shown in figure 7. When the curve is inspected with diameter ratio as the variable, and the aspect ratio, solidity, and stress ratio constant, it can be seen that a careful consideration of diameter ratio is necessary if the weight of a wheel is to be kept low. It will be noted in this particular case that wheel weight increases very rapidly when the diameter ratio is increased beyond about 0.70, and that an increase in diameter ratio from 0.70 to 0.80 more than doubles the weight of the wheel. As in the case of disk weight, however, increasing the diameter ratio and maintaining the stress at the blade root constant increases the allowable tip velocity.

In the calculation of wheel weight with aspect ratio as the variable and all the other factors maintained constant, the effect is primarily that of changing the thickness of the wheel. Inasmuch as solidity is constant, the number of blades will change. It may be noted that in this case doubling the aspect ratio from 1.5 to 3.0 more than halves the weight of the wheel, and that wheel weight is approximately inversely proportional to aspect ratio.

Maintaining solidity, aspect ratio, and diameter ratio constant and varying stress ratio from 0.7 to 1.1 causes a wheel-weight increase of 39 percent.

Solidity had less effect on total wheel weight than any of the other three variables. For a solidity change from 1.25 to 2.00, the wheel weight varies 17 percent.

A comparison of calculated weights and actual weights of some current turbine wheels is presented in figure 8. The values for the variables and constants used in these calculations are shown in the following table:

Wheel	Measured from wheel						Estimated			
	A (sq ft)	l (ft)	β	D_i/D_o	δ	σ	s_b/s_d	f	ρ_b (lb/cu ft)	ρ_d (lb/cu ft)
1	0.802	0.221	5.230	0.680	2.172	1.511	0.900	0.3	540	510
2	1.920	.333	5.515	.692	2.000	1.720	.900	.3	540	510
3	1.965	.375	4.450	.634	2.769	1.393	.900	.3	540	510
4	1.439	.326	4.310	.625	3.207	1.262	.900	.3	540	510
5	1.439	.326	4.310	.625	2.778	.900	.900	.3	540	510
6	.853	.224	5.415	.688	2.680	1.314	.900	.3	540	510
7	.296	.100	9.425	.807	2.733	1.762	.900	.3	540	510

Except for the lightest wheel, all of the calculated wheel weights average about 15 pounds less than the actual wheel weights.

Figure 9 may be considered a design chart in which the values of solidity, stress ratio, and density chosen for design are kept constant, and the effect of a varying annulus area and blade length on wheel weight per unit of annulus area is investigated. Included in the plot are lines of constant diameter ratio. For geometrically similar wheels, the wheel weight per unit of annulus area is less for small wheels than it is for large wheels. It will be noted that this effect is minimized at the lower diameter ratios.

SUMMARY OF RESULTS

A study has been made of the effect of changes in aspect ratio, solidity, diameter ratio, and stress ratio on the weight of a turbine wheel. The aspect ratio, solidity, and diameter ratio are, in general, fixed by the aerodynamic and thermodynamic specifications of the turbine-wheel design, and the stress ratio by the quality of the materials to be used. The effect of these variables on turbine efficiency and their choice and variation with the aerodynamic and thermodynamic characteristics of the turbine design have not been considered in this analysis.

Equations have been developed for the calculation of disk, blade, and rim weights for a wheel model having a disk profile of the de Laval type. The effect of blading aspect ratio and solidity, stress ratio, and diameter ratio on these wheel components, assuming a blade whose cross-sectional area varies linearly from root to tip, has been shown. Figures have been presented and equations developed whereby blades with cross-sectional area distributions other than linear may be considered.

From the curves presented, it is seen that for a given annulus area, wheel weight was very sensitive to diameter ratio. In the region of high diameter ratios, the wheel weight increased very rapidly with an increase in diameter ratio. This effect was also observed from inspection of the disk- and blade-weight equations in which it is noted that both disk and blade weight are directly dependent upon blade length.

Increases in stress ratio and in blade solidity increased the total wheel weight, the stress ratio having a greater effect on the total wheel weight than the solidity.

An increase in blade aspect ratio decreased wheel weight, wheel weight being approximately inversely proportional to aspect ratio.

A curve of the actual weights of some current turbine wheels plotted against calculated wheel weights using the method of this report showed that a good correlation exists between the actual and theoretical wheel weights.

A chart showing the variation in total wheel weight with changes in annulus area and in blade length was constructed for obtaining approximate turbine wheel weights for a fixed set of values for disk and blade density, stress ratio, and blade solidity.

Lewis Flight Propulsion Laboratory,
National Advisory Committee for Aeronautics,
Cleveland, Ohio, December 9, 1948.

REFERENCES

1. Howell, A. R.: Design of Axial Compressors. War Emergency Issue No. 12 pub. by Inst. Mech. Eng. (London), 1945. (Reprinted in U.S. by A.S.M.E., Jan. 1947, pp. 452-462.)

2. Stodola, A.: Steam and Gas Turbines. Vol. I. McGraw-Hill Book Co., Inc., 1927, pp. 372-379. (Reprinted, Peter Smith (New York), 1945.)

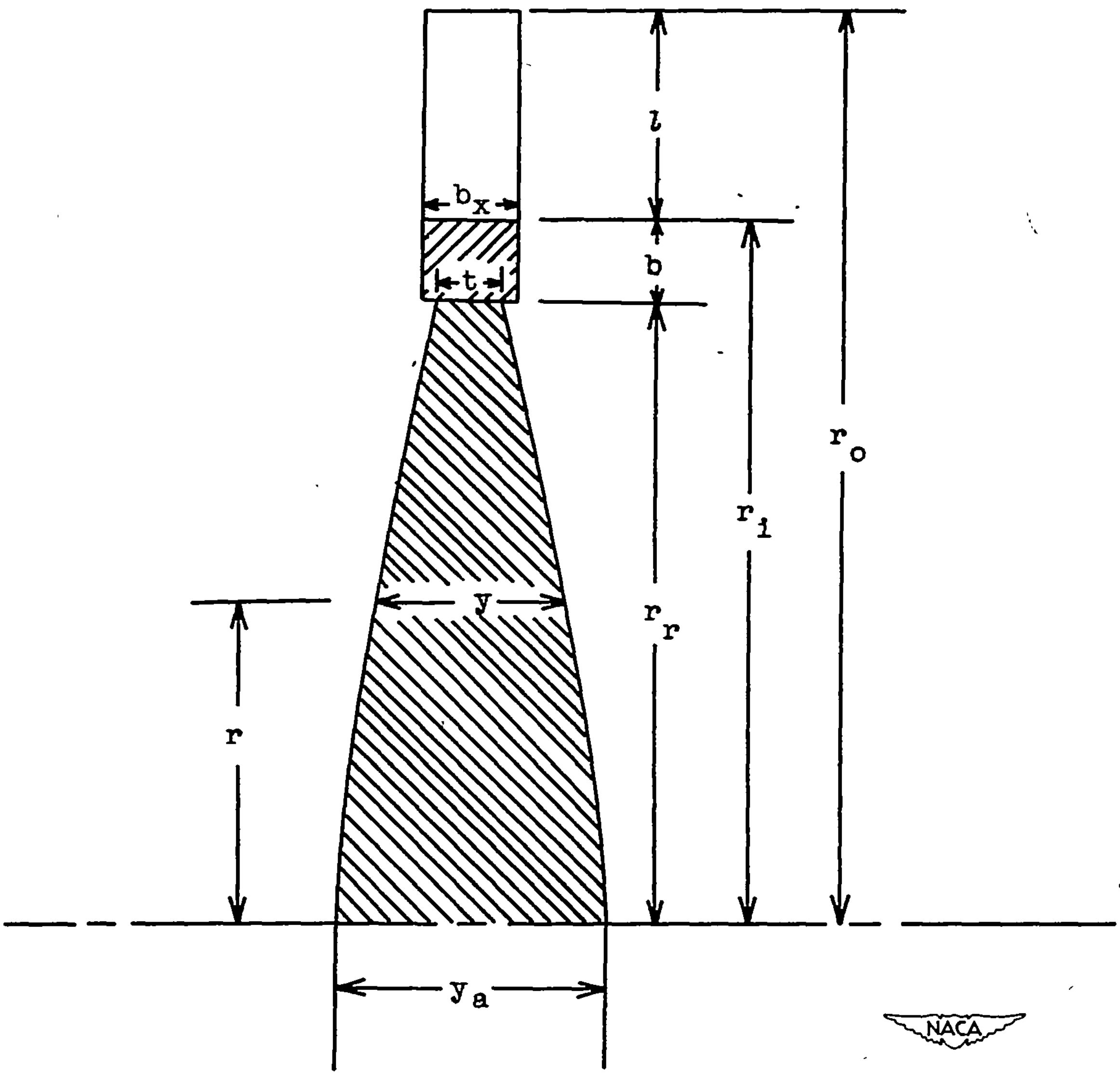

Figure 1. - Wheel model and nomenclature for analysis.

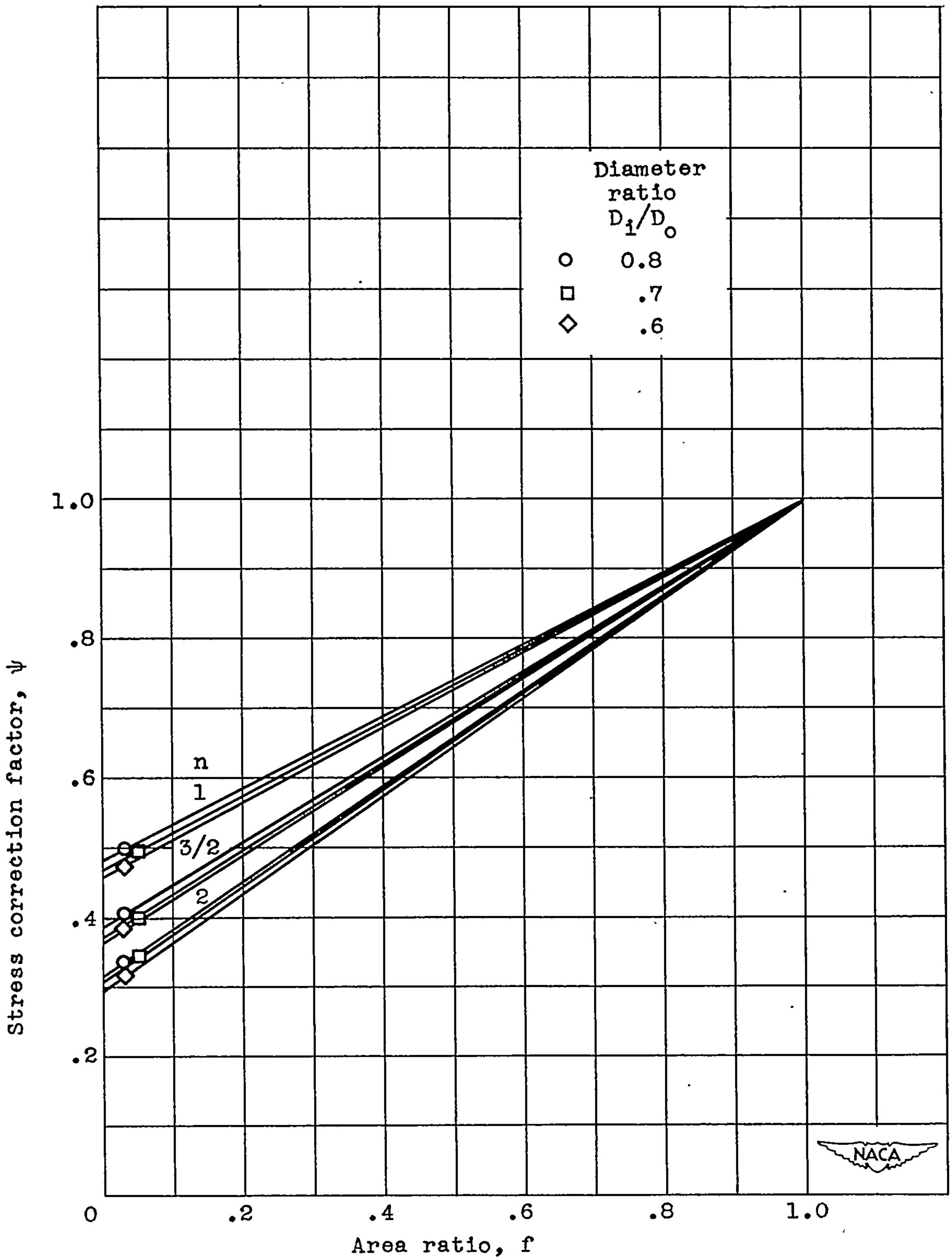

Figure 2. - Chart for determining stress correction factor for tapered blades. Blade density ρ_b, 540 pounds per cubic foot.

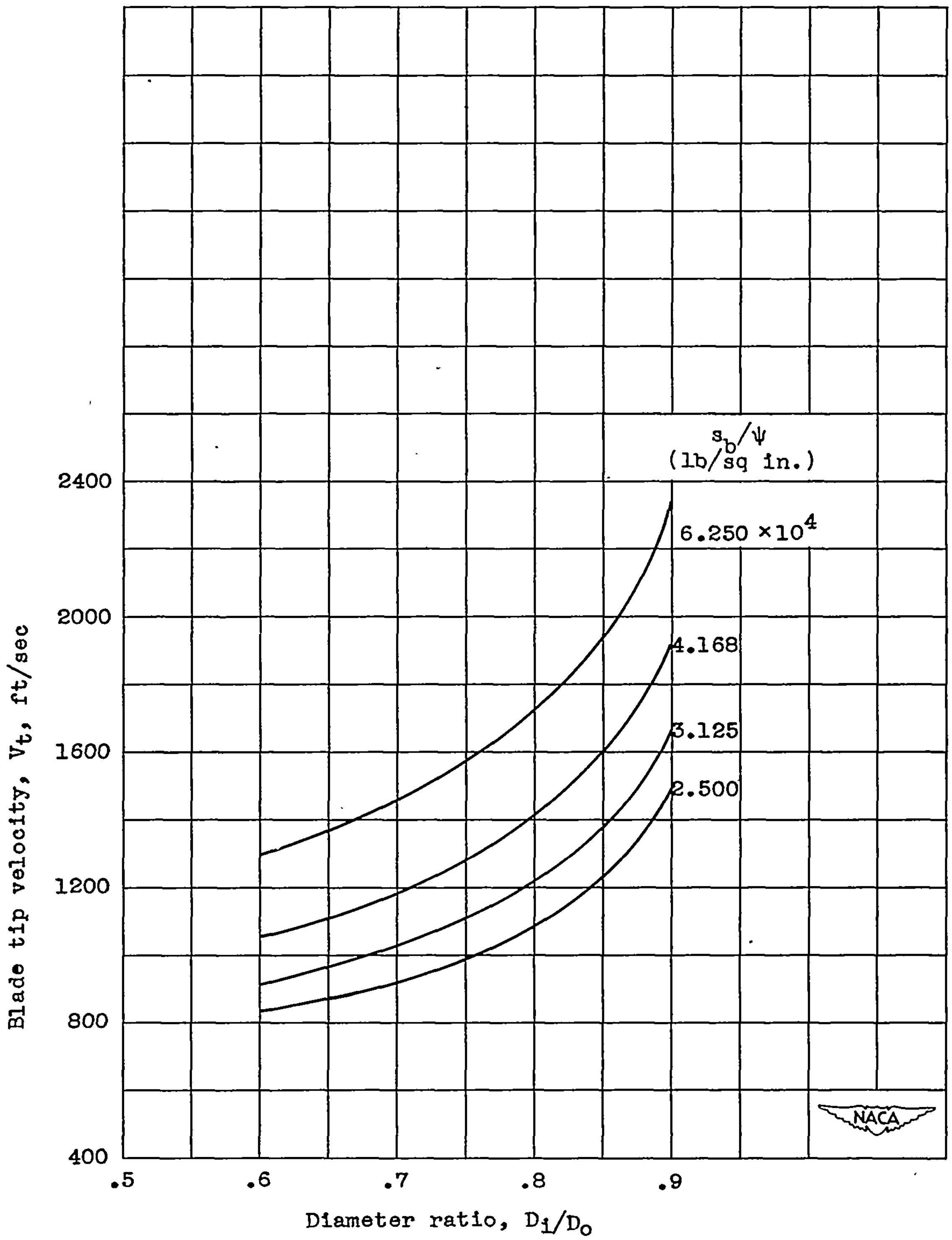

Figure 3. - Chart for determining blade tip velocity. Blade density ρ_b, 540 pounds per cubic foot.

1064

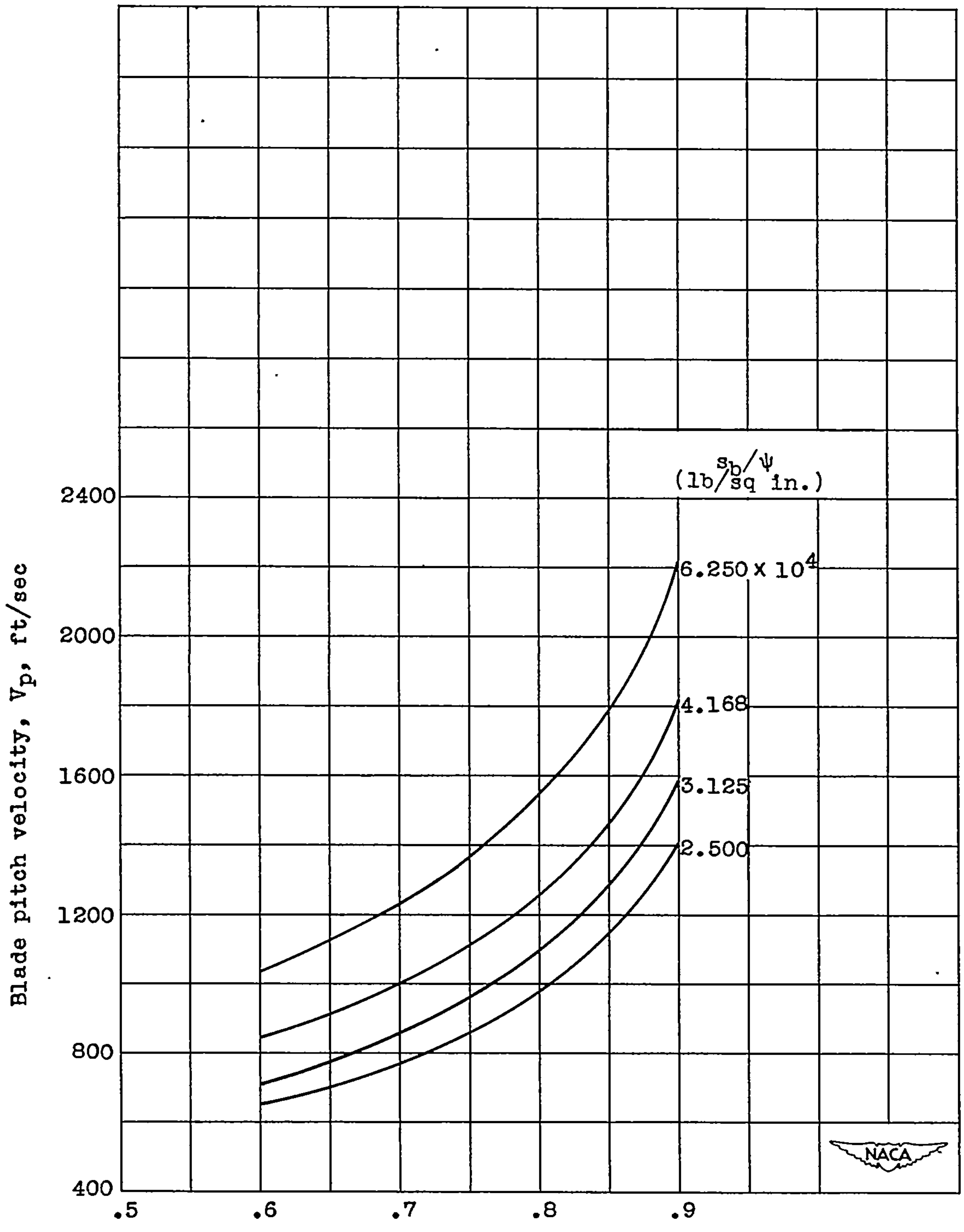

Figure 4. - Chart for determining blade pitch velocity. Blade density ρ_b, 540 pounds per cubic foot.

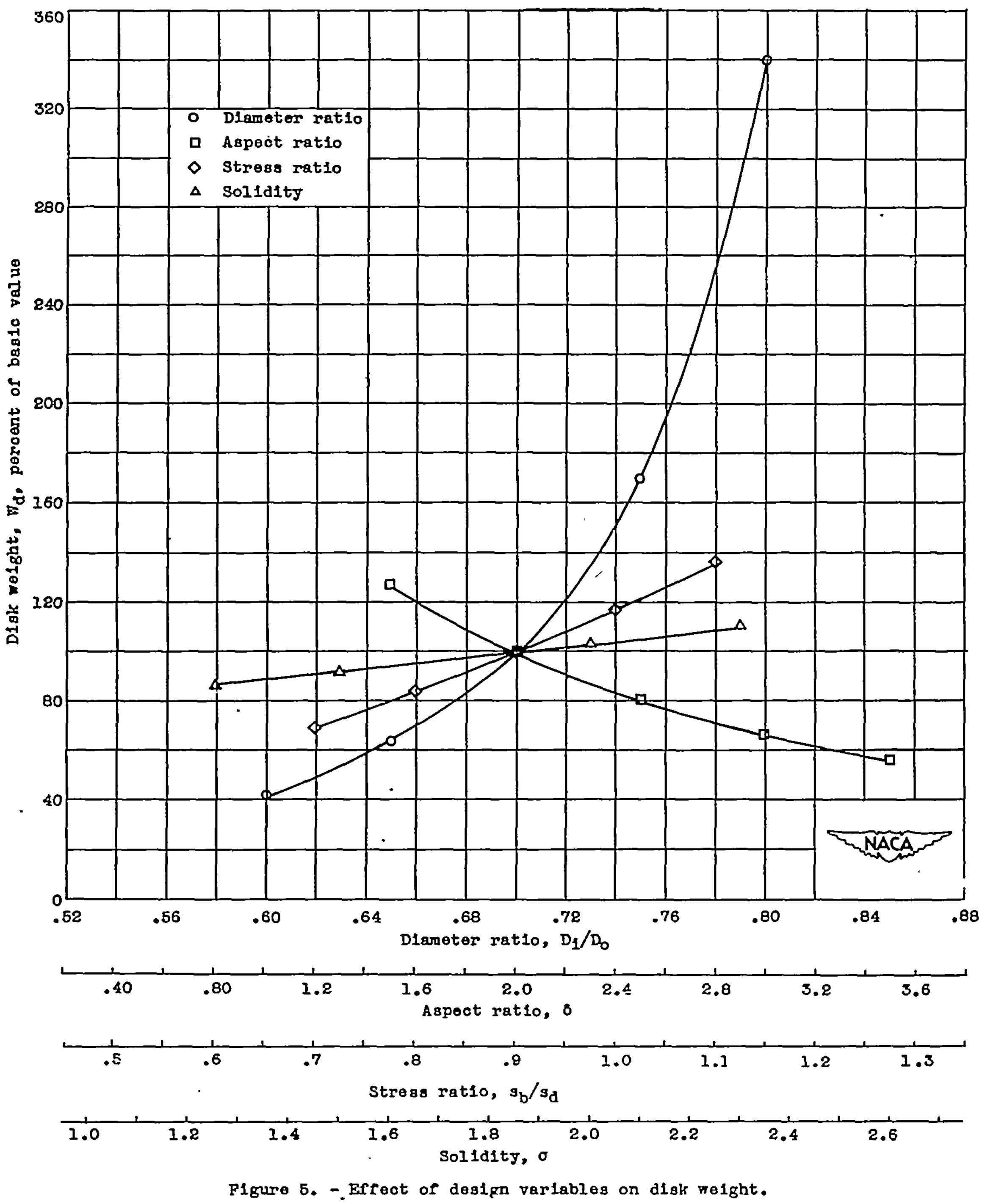

Figure 5. - Effect of design variables on disk weight.

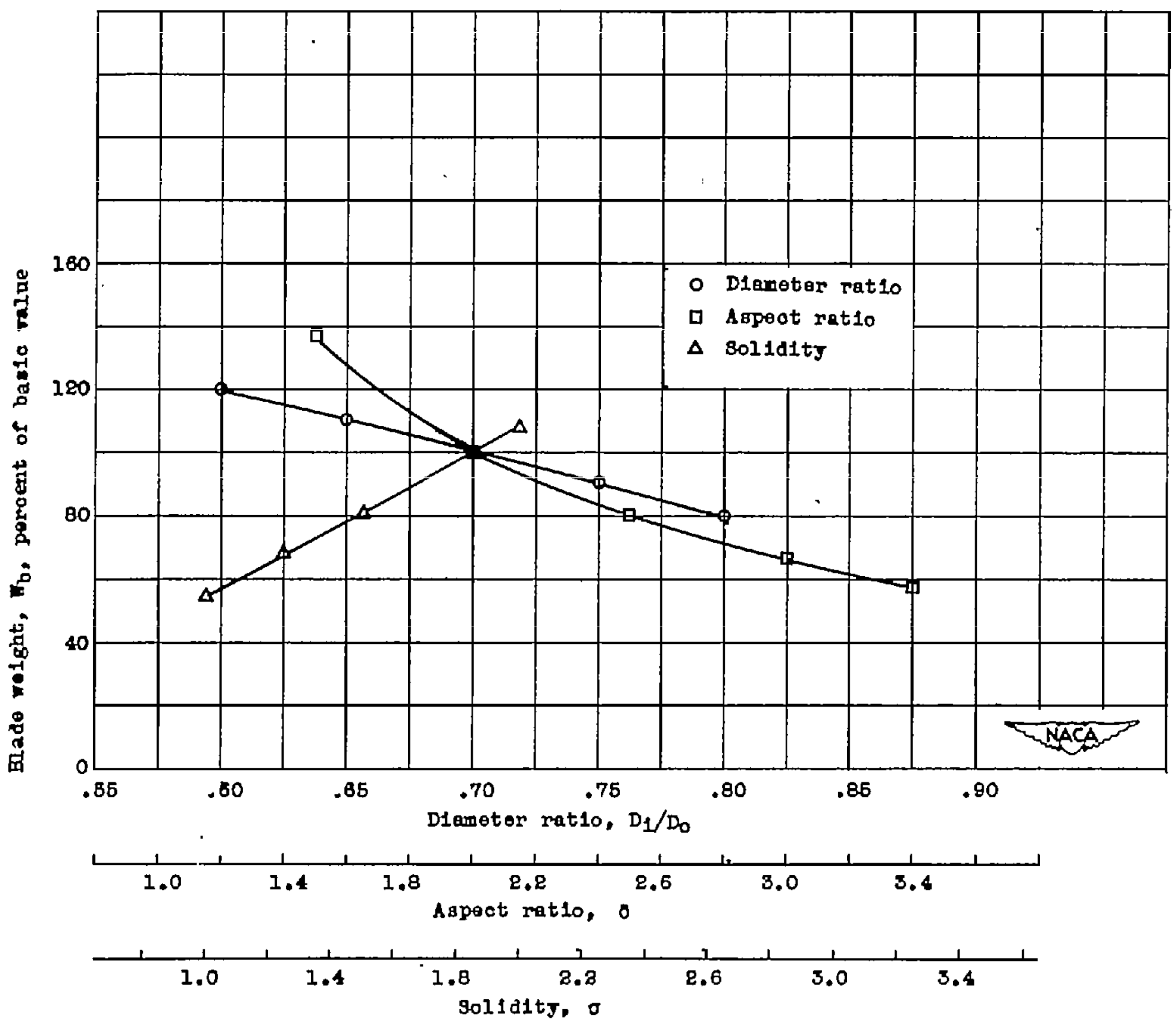

Figure 6. - Effect of design variables on blade weight.

1064

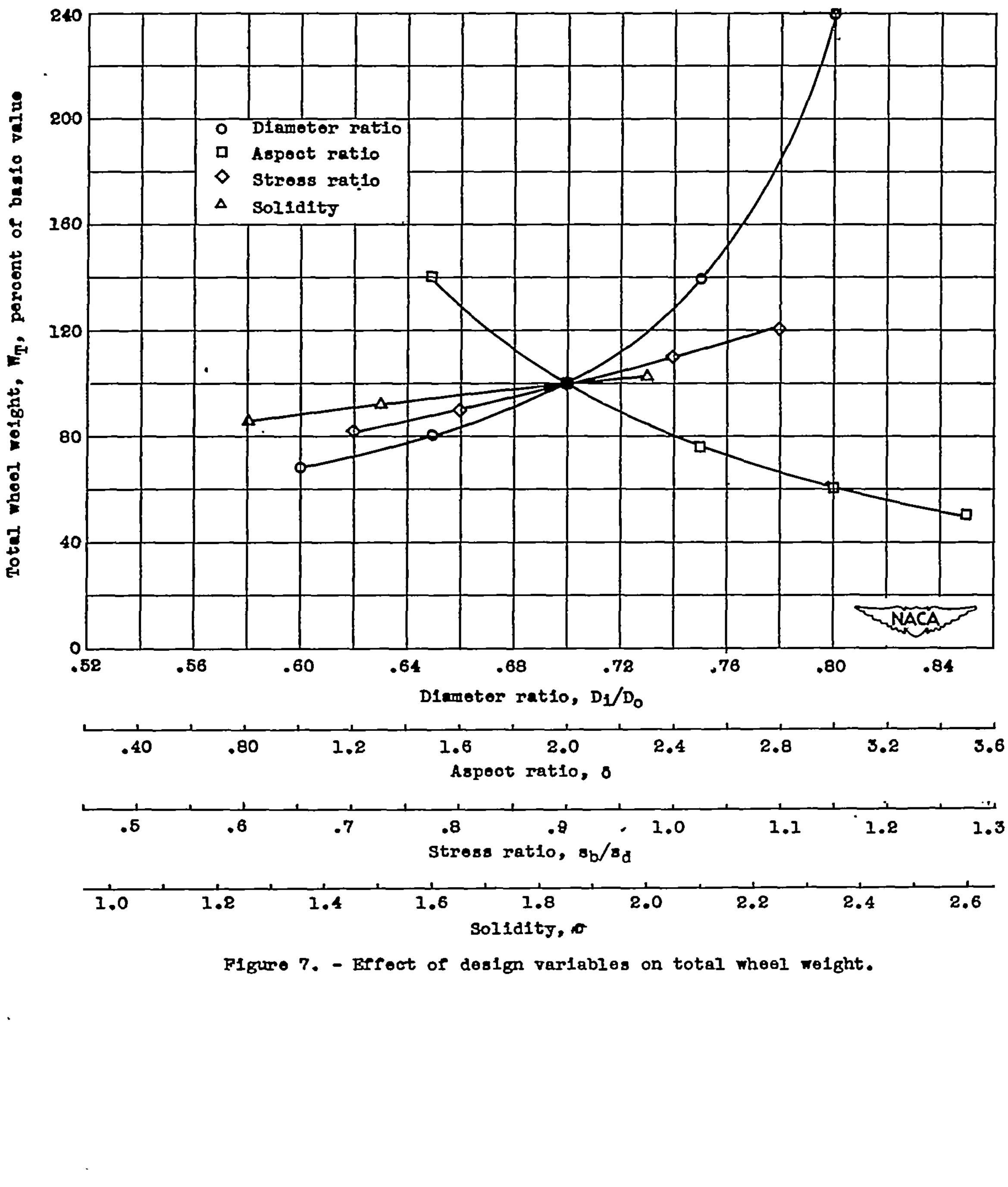

Figure 7. - Effect of design variables on total wheel weight.

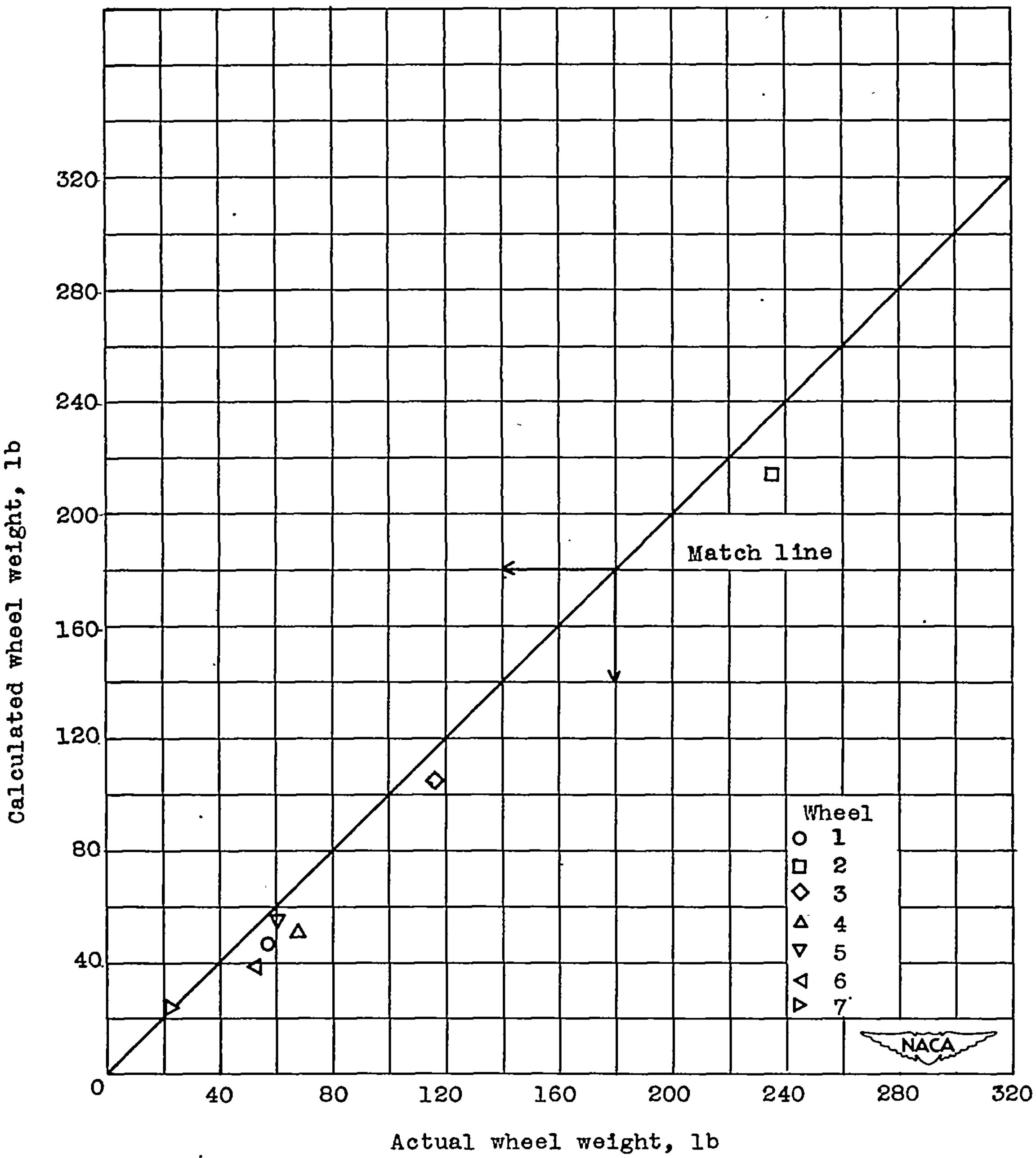

Figure 8. - Comparison of calculated and actual wheel weights.

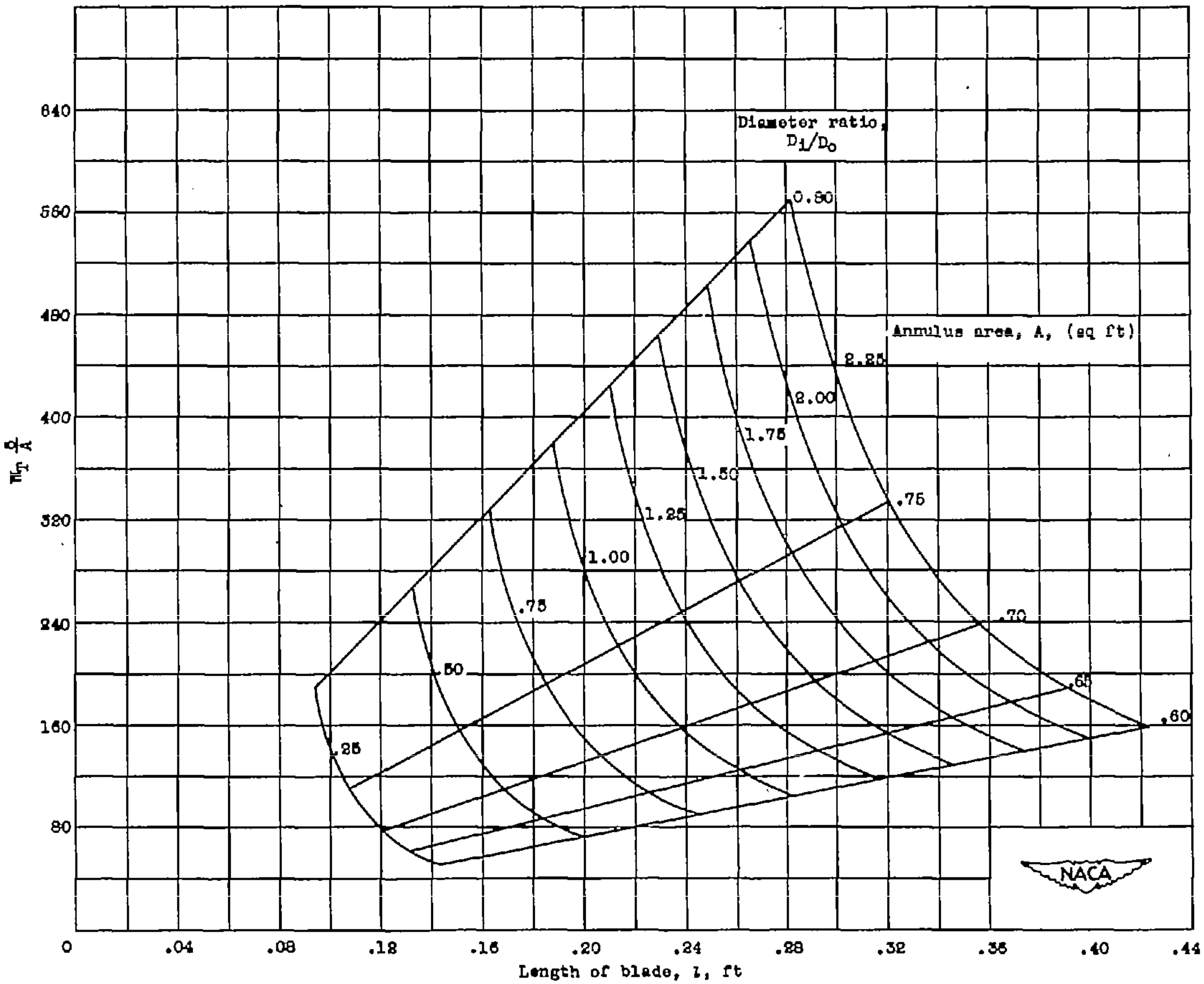

Figure 9. - Weight chart. Stress ratio s_b/s_d, 0.900; solidity σ, 1.500; area ratio f, 0.300; proportionality constant K, 0.150; disk density ρ_d, 510 pounds per cubic foot; blade density ρ_b, 540 pounds per cubic foot.